Chapter 6 22 December 2003, M=6.5 San Simeon, California, earthquake

The $M = 6.5$ San Simeon earthquake occurred on 22 December 2003 on a blind thrust fault in the central coast of California. The mainshock nucleated at $35.702°N, 121.08°W$ at a depth of 7 km and propagated unilaterally to the southeast (Hardebeck et al., 2004). There were two casualties in the town of Paso Robles, located about 39 km away from the epicenter and in the forward directivity direction.

The San Simeon earthquake occurred along the boundary of the reporting regions of the Southern California Seismic Network (SCSN) and the Berkeley Digital Seismic Network (BDSN). While there is a dense USGS strong motion array to monitor the Parkfield area, the density of broadband, high-dynamic range stations with real-time telemetry is sparse relative to the more heavily instrumented regions of the seismic network. The stations closest to the epicenter were PKD (BDSN) and PHL (SCSN), at distances of 57 and 61 km, respectively.

6.1 Road map

Application of the VS method for early warning on the San Simeon dataset illustrates how the method performs for larger events along the outer edges of the network. Station geometry, previously observed seismicity, the San Andreas fault trace, and the Gutenberg-Richter magnitude-frequency relationship are included in the Bayes prior. Following some comments on station geometry in Central California, the VS single station estimate (using the available amplitudes at the first triggered station, PKD, 3 seconds after the initial P detection) are discussed. The effects of different Bayes priors (with and without the Gutenberg-Richter relationship) are evaluated. Updated VS estimates at 5.5, 8, 11, 31, and 71 seconds after the initial P detection are discussed.

The constraints from not-arrived data are illustrated. The amplitude-based location (or strong motion centroid), and how the observed amplitudes behaved relative to the expected levels of ground motion from the envelope attenuation relationships in Chapter 2 will be presented.

6.2 Station geometry in Central California

Figure 6.1 shows the operating SCSN/BDSN stations within 250 km of the epicenter of the M=6.5 San Simeon mainshock. The polygons define the nearest neighbor regions of the stations about which they are centered. If station A has the first P detection from a event, the earthquake is constrained to be located within station A's Voronoi cell. The first triggered station is PKD (Parkfield), located about 57 km away from the epicenter. PKD's Voronoi cell is shaded in Figure 6.1. The Voronoi cells around the epicentral region are relatively large, due to the low density of stations with high dynamic range and real-time telemetry in this region. Table 6.1 lists the locations, Voronoi areas, epicentral distance, fault distance, and P wave arrival times at PKD and stations sharing a Voronoi edge with PKD. The Voronoi areas of stations at Rector (RCT) and the San Andreas Geophysical Observatory (SAO) are characteristic of station along the outer boundaries of the network. The locations of $M \geq 1$ earthquakes located by the network in the 24 hours preceding the mainshock are marked by circles. Two of these were located (by BDSN) within PKD's Voronoi cell - an M=1.18 event on the San Andreas and an M=1.22 event within 8.5 km of the mainshock epicenter. Of course, there is no way (thus far) to distinguish between a foreshock and a non-foreshock without a mainshock.

Figure 6.2 shows the observed vertical acceleration records from PKD and the stations which share a Voronoi edge with PKD. The P arrivals at PKD and PHL are very closely spaced - about 1.06 seconds apart. Since the first two P arrivals are practically simultaneous, the epicenter must lie somewhere close to the Voronoi boundary shared by PKD and PHL. The vertical lines marked "T0" and "T1" are the theoretical P and S wave travel times given the reported location for the epicenter of

$35.71°N, 121.10°W$.

Stations surrounding the epicenter of the 2004 $M = 6.5$ San Simeon mainshock

Station name	Abrev	Lon	Lat	vor. area km^2	ep. dist. km	fault dist. km	P-Arrv. sec
Parkfield	PKD	-120.542	35.945	13,269	57.2	44.81	9.35
Park Hill	PHL	-120.546	35.408	18,379	60.7	31.4	10.4
Simmler	SMM	-119.996	35.314	4,318	109.7	79.5	18.14
SanAndr.Obs	SAO	-121.447	36.764	37,226	121.1	121.1	19.9
Rector	RCT	-119.244	36.305	101,630	180.32	159.8	28.3
Vestal	VES	-119.085	35.841	3,744	183.2	156.8	28.7

Table 6.1: Stations surrounding the epicenter of the 2003 M=6.5 San Simeon mainshock. The station closest to the epicenter is Parkfield (PKD), at an epicentral distance of 57.2 km. Stations SAO and RCT have Voronoi cells with very large areas; this is characteristic of stations along the outer boundaries of the seismic network.

6.3 Single station estimates: solving for magnitude and epicentral distance

With data from a single station, the VS method can be used to solve for either 1) magnitude and epicentral distance or 2) magnitude and epicentral location. The VS estimates for magnitude and epicentral distance using the first 3 seconds of data after the P detection at PKD are presented first.

Let Z.a, Z.v, and Z.d refer to the maximum vertical acceleration, velocity, and filtered displacement amplitudes observed at a given station between the P detection and some time t. EN.a, EN.v, and EN.d are the corresponding envelope amplitudes for the root mean square of the horizontal channels.

Figure 6.3 (a) shows the P/S discriminant function (discussed in Appendix C) as a function of time. The P/S discriminant function is $PS = 0.4\log_{10}(Z.a_{max}) + 0.55\log_{10}(Z.v_{max}) - 0.46\log_{10}(EN.a_{max}) - 0.55\log_{10}(EN.v_{max})$, where the subscript max refers to the peak amplitude on a given channel from the time of the initial P detection to some given time. The first time P/S becomes negative after the

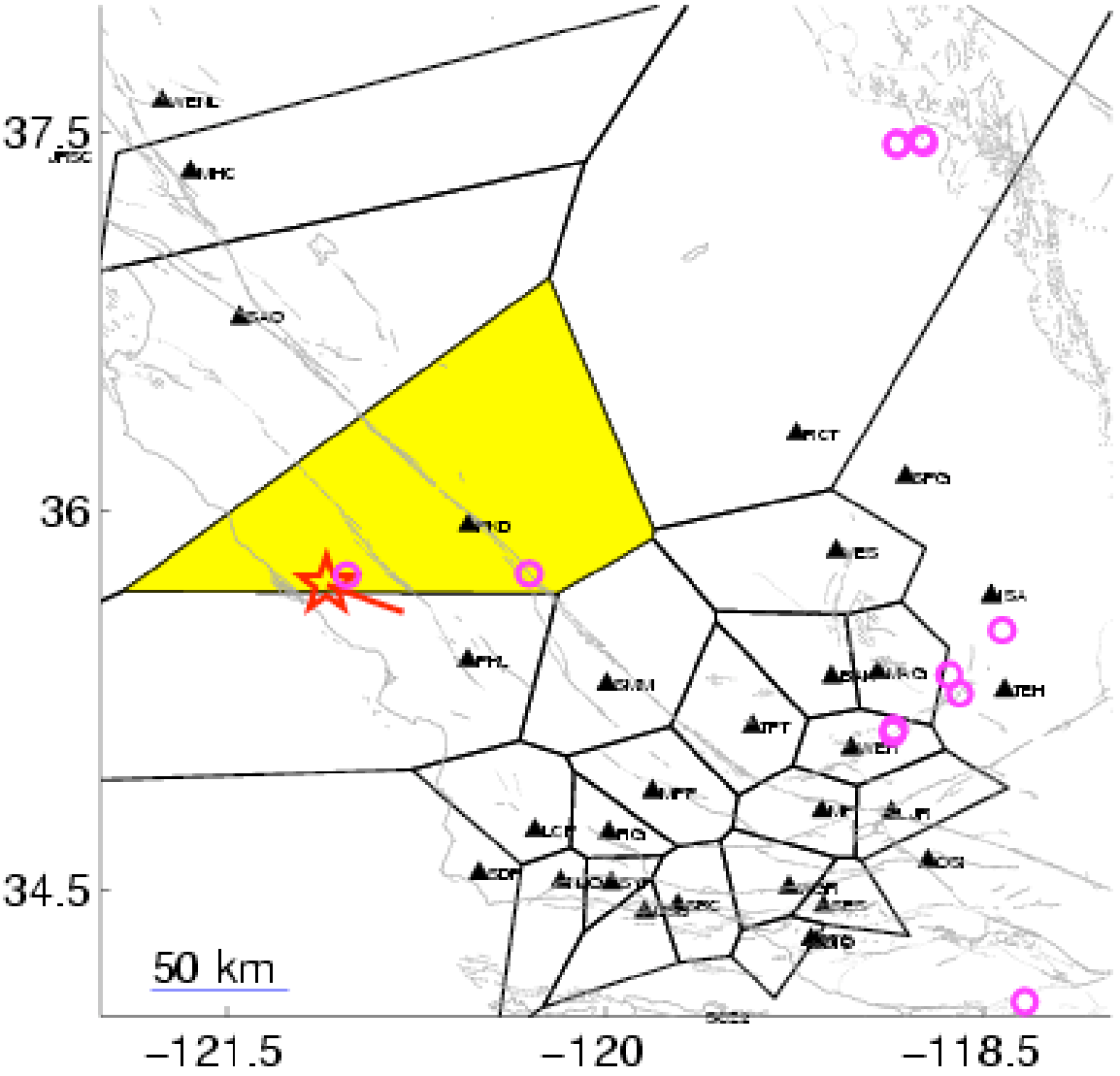

Figure 6.1: Voronoi cells of stations within 250 km of San Simeon earthquake. Triangles denote station locations. Circles mark the location of earthquakes with magnitudes $M \geq 1$ recorded in the 24 hours preceding the $M = 6.5$ San Simeon mainshock. There were 12 such events located in the region bounded by latitudes $34°N$ and $37.5°N$ and longitudes $121°W$ and $118°W$; two of which are located in the Voronoi cell of PKD, the station closest to the mainshock epicenter.

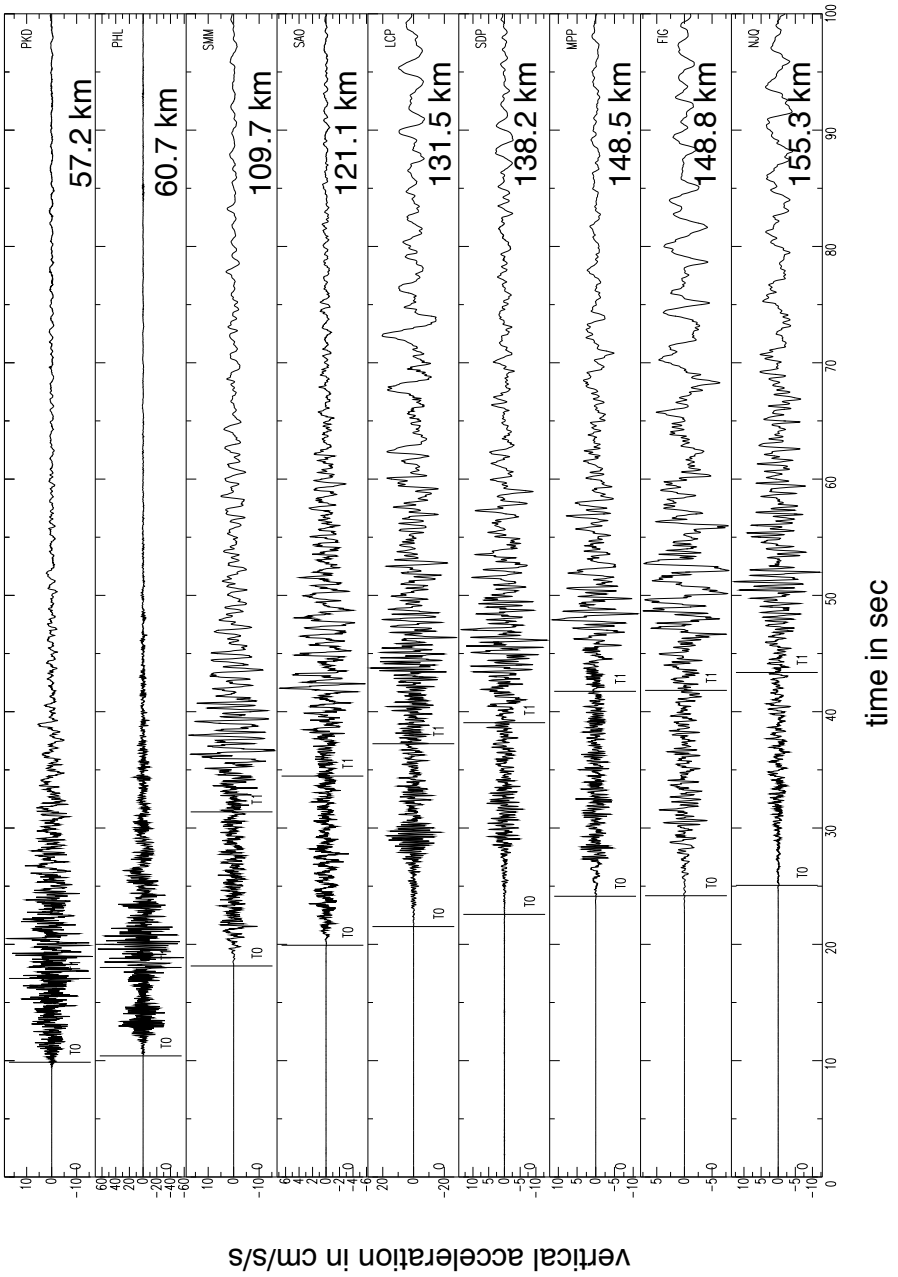

Figure 6.2: Vertical acceleration records from stations sharing a Voronoi edge with the first triggered station, PKD. Vertical lines marked "T0" and "T1" are the predicted P and S arrival times using Eaton's travel time code, a 6 layer, 1 D Southern California velocity model, and the SCSN-reported location of $35.71°N, 121.10°W$.

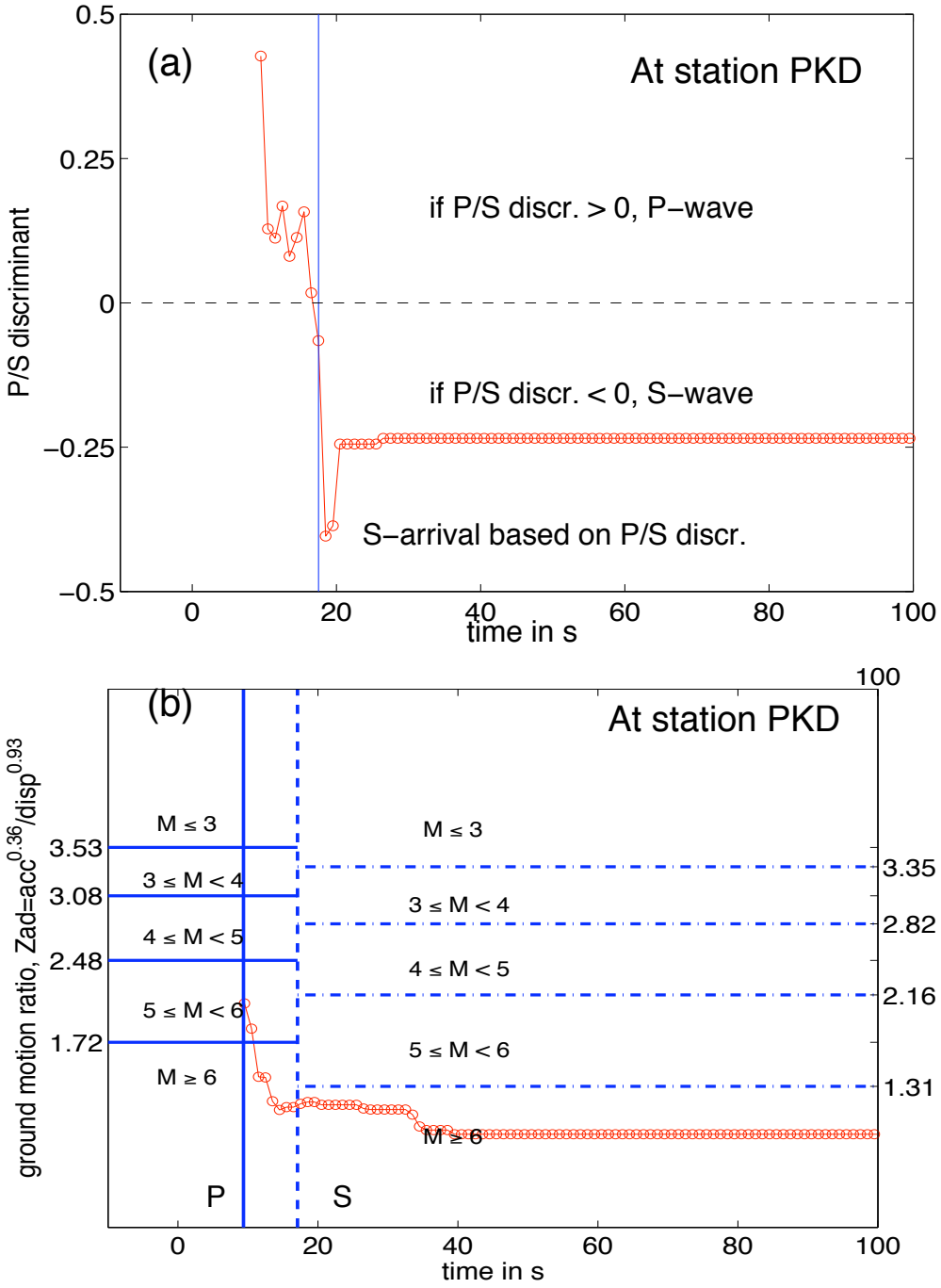

Figure 6.3: (a) The P/S discriminant $PS = 0.43\log_{10}(Z.a) + 0.55\log_{10}(Z.v) - 0.46\log_{10}(EN.a) - 0.55\log_{10}(EN.v)$ at PKD as a function of time. The first zero crossing of PS *after* the P arrival indicates the S arrival. The P/S discriminant puts the estimated S-wave arrival about 2 seconds after the predicted arrival time using the SCSN-reported location. (b) The ground motion ratio $Z_{ad} = \frac{Z.a^{0.36}}{Z.d^{0.93}}$ as a function of time. The decision boundaries on the left-hand side are for P-wave amplitudes; those on the right-hand side for S-wave amplitudes. The vertical ground motion ratios consistently indicate that the event is $M \geq 6$.

P arrival marks the S-wave arrival. Figure 6.3 (b) shows the ground motion ratio $Z_{ad} = Z.a^{0.36}/Z.d^{0.93} = 0.36\log_{10}(Z.a) - 0.93\log_{10}(Z.d)$ as a function of time. The left-hand axis shows the P-wave decision boundaries; those on the right, the S-wave decision boundaries. The ground motion ratio, Z_{ad}, from the first 3 seconds of data at PKD indicate that the event is in the group $M \geq 6$.

The likelihood function (Eqn. 4.62) combines the magnitude estimates from the vertical acceleration and displacement ground motion ratio, along with the peak available vertical velocity, and rms horizontal acceleration, velocity, and displacement amplitudes to estimate magnitude and epicentral distance. Figure 6.4 shows contours of the likelihood function expressed in terms of M and R. The likelihood is scaled to have a maximum value of 1; contours are drawn at the 0.6, 0.1, and 0.01 levels, which correspond to $\pm 1\sigma$, $\pm 2\sigma$, and $\pm 3\sigma$ about the mean of a 1-d Gaussian pdf. The "high" probability region within the 0.6 level contour is shaded; the actual magnitude and epicentral distance (star) is near this region. Trade-offs between M and R cannot be resolved by the 3 second observations; this is evident from the elongated contours of the likelihood function. While trade-offs exist, the likelihood function does have a peak. An M=6.7 event 158 km away from PKD maximizes the likelihood function based on available peak amplitudes at PKD 3 seconds after the P detection. The San Simeon mainshock had magnitude M=6.5 and an epicenter 57 km away from PKD.

When expressing the problem in terms of magnitude and epicentral distance, the only prior information ("prior" in that they do not involve the observed amplitudes) that can be included are 1) the range of epicentral distances consistent with the Voronoi cell of the first triggered station and 2) the Gutenberg-Richter magnitude-frequency relationship. Assuming that all locations within PKD's Voronoi cell are equally likely to be the epicenter, certain epicentral distances will be better represented than others. A probability density function for epicentral distances within PKD's Voronoi cell can be constructed. In Figure 6.5, the solid line (black) shows the pdf of epicentral distances (scaled to a maximum value of 1) consistent with a first arrival at station PKD. There are near-simultaneous arrivals (about 1 second apart) at PKD and PHL. Taking into account the time interval between the first two

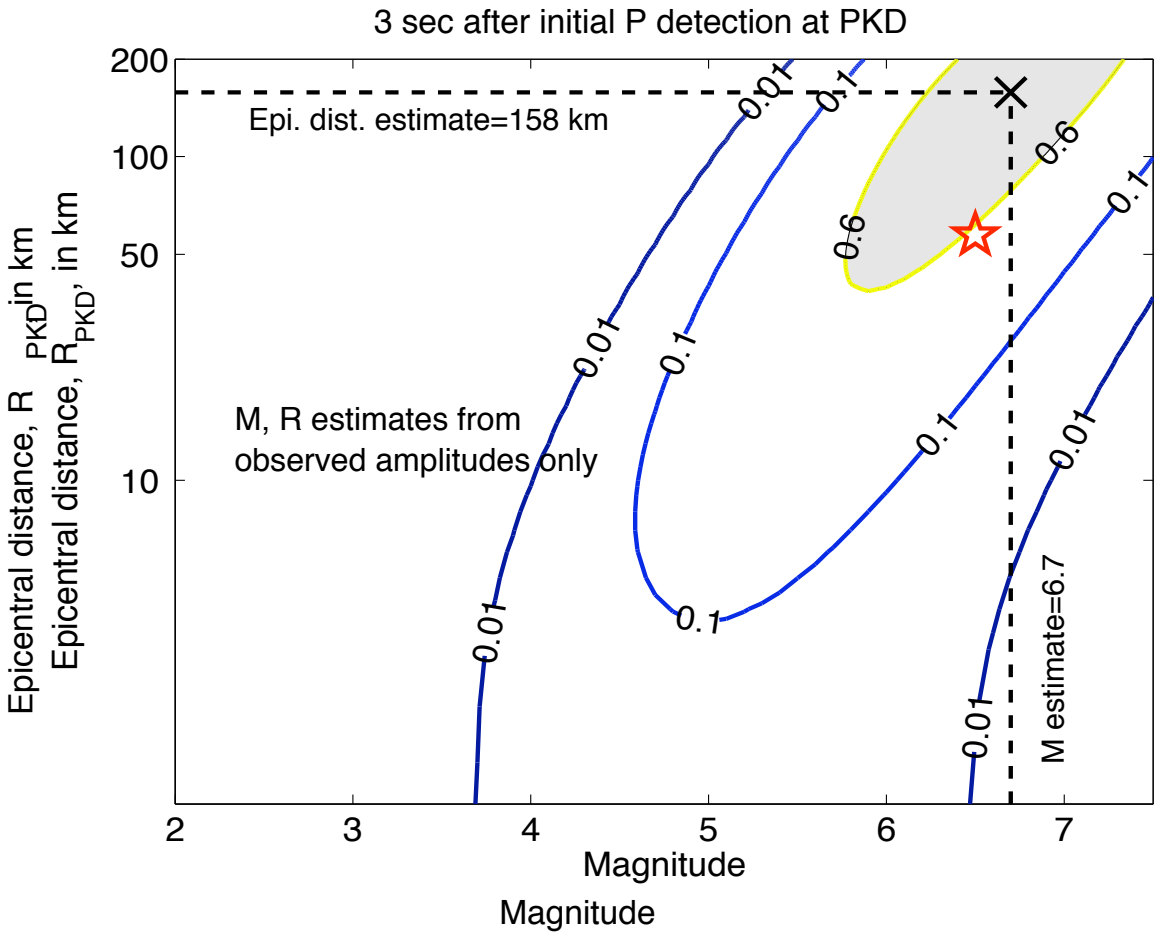

Figure 6.4: Contours of the likelihood function (expressed in terms of magnitude and epicentral distance) given the amplitudes at PKD 3 seconds after the initial P detection. Contours are drawn at 0.6, 0.1, 0.01 levels. Regions where the likelihood function has value ≥ 0.6 are shaded.

P arrivals (red dashed line) does not have much effect on the epicentral distance pdf.

At the time of the initial VS estimate, the available amplitudes (and arrivals) are not able to fully resolve the trade-offs between magnitude and distance, as evidenced by the elongated contours of the likelihood function in Figure 6.4. The shape of the Bayes posterior density function, whose maxima correspond to the VS estimates, will depend on the form of the prior. From Figure 6.5, whether or not the second arrival at PHL is taken into account makes no appreciable difference in the epicentral distance pdf. However, whether or not the Gutenberg-Richter magnitude frequency relationship is used makes a considerable difference in the resulting VS estimates. This is shown in Figure 6.6. Using the Gutenberg-Richter (G-R) relationship resolves the trade-offs in the likelihood in favor of smaller magnitudes at closer distances to the station. Without the G-R, the VS estimate is a magnitude $5.5 \leq M \leq 6.5$ earthquake located about 50 km from PKD; with the G-R, the corresponding estimate is a magnitude $4.5 \leq M < 5.5$ event located about 30 km from the station. Note: in Figure 6.6, the likelihood does *not* include the amplitudes at PHL, since there is less than 3 seconds of data available there.

6.4 Multiple station estimates: solving for magnitude and epicentral location

Updating the VS estimates as the ground motions propagate to further stations is more convenient when the problem is expressed in terms of magnitude and epicentral location (latitude and longitude). This change in coordinate system also allows information about fault locations and previously observed seismicity to be included in the Bayes prior.

Figure 6.7 shows the contours of the P-wave wavefront at the times of various VS estimates- at 3, 5.5, 8, 11, 31, and 71 seconds after the initial P detection (add 9.5 seconds to get VS estimate times relative to earthquake origin time).

From Figure 6.7, at t=17.5 sec after the origin time, the P waves have not yet

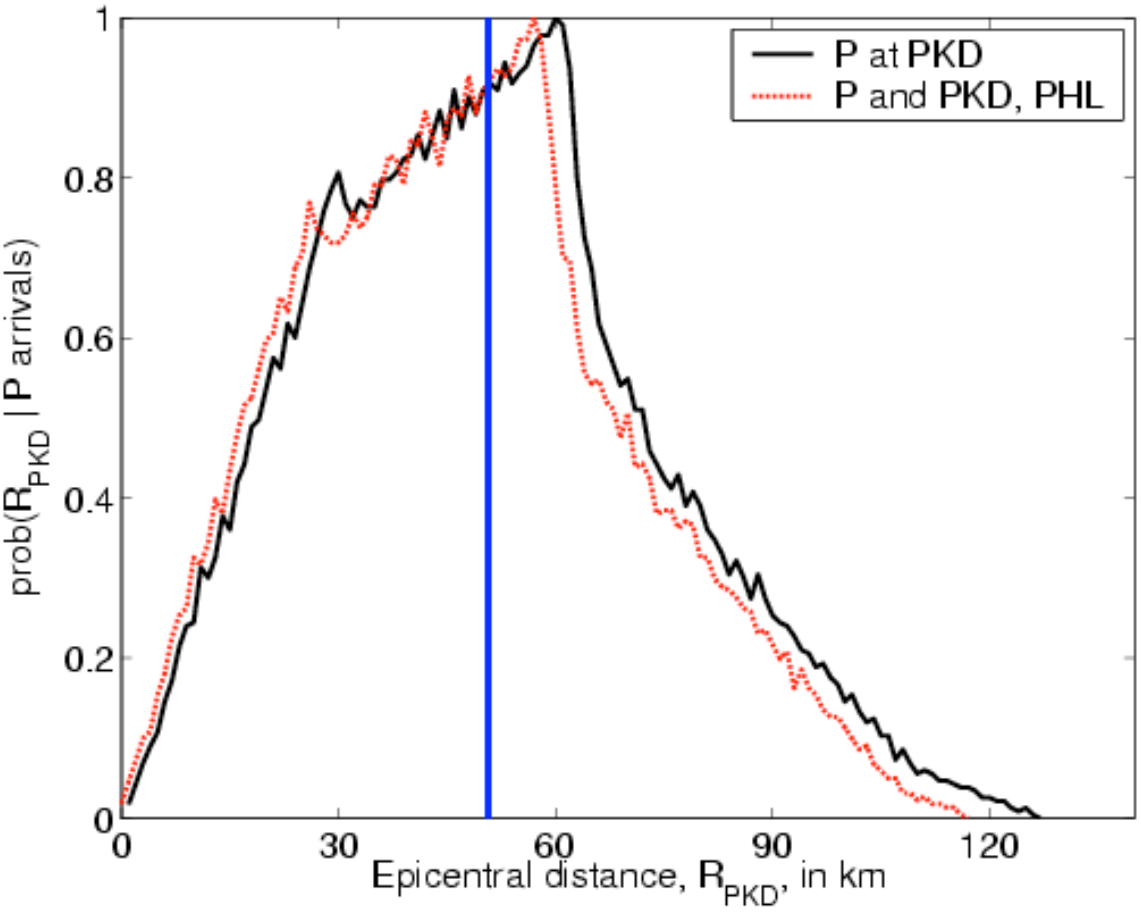

Figure 6.5: The range of possible epicentral distances, R_{PKD} with 1) the first P arrival at PKD (solid line) and 2) the time interval between the first two arrivals (dashed line). The vertical line shows the epicentral distance to PKD calculated using the SCSN-reported location. The possible epicentral distances to PKD from the station geometry (solid line) is truly prior information. Such curves can be easily calculated and updated for all stations each time a station is put on- or taken off-line. The possible epicentral distances to PKD given the first two P arrivals is not strictly prior information, since the interval between the arrivals at PKD and PHL is an observed quantity.

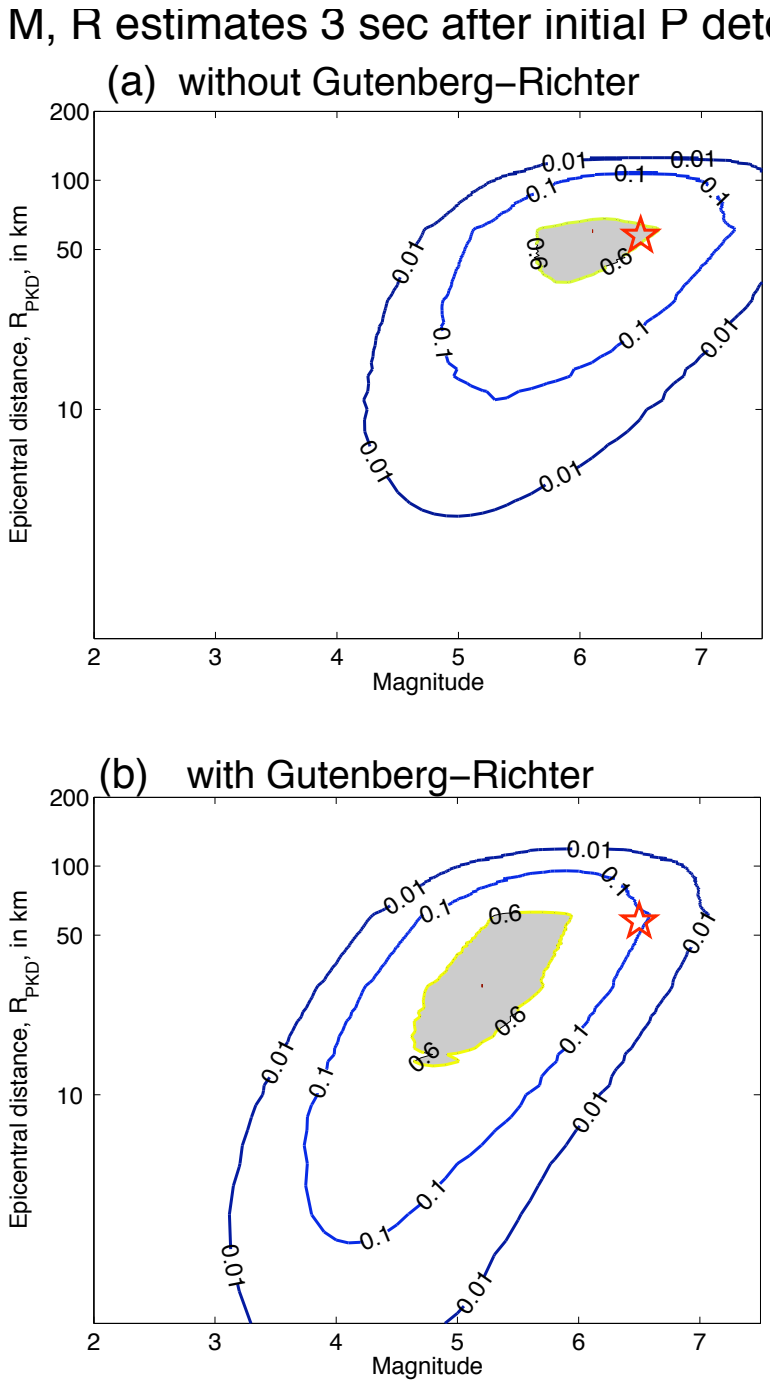

Figure 6.6: The effects of including the Gutenberg-Richter magnitude-frequency relationship on the Bayes posterior $prob(M, R|data)$, and hence, the VS estimates, 3 seconds after the initial P detection at PKD. Regions in M-R space where $prob(M, R|data) \geq 0.6$ are shaded. If the Gutenberg-Richter relationship is *not* included in the Bayes prior, the "high" probability shaded region includes the actual magnitude and epicentral distance (star).

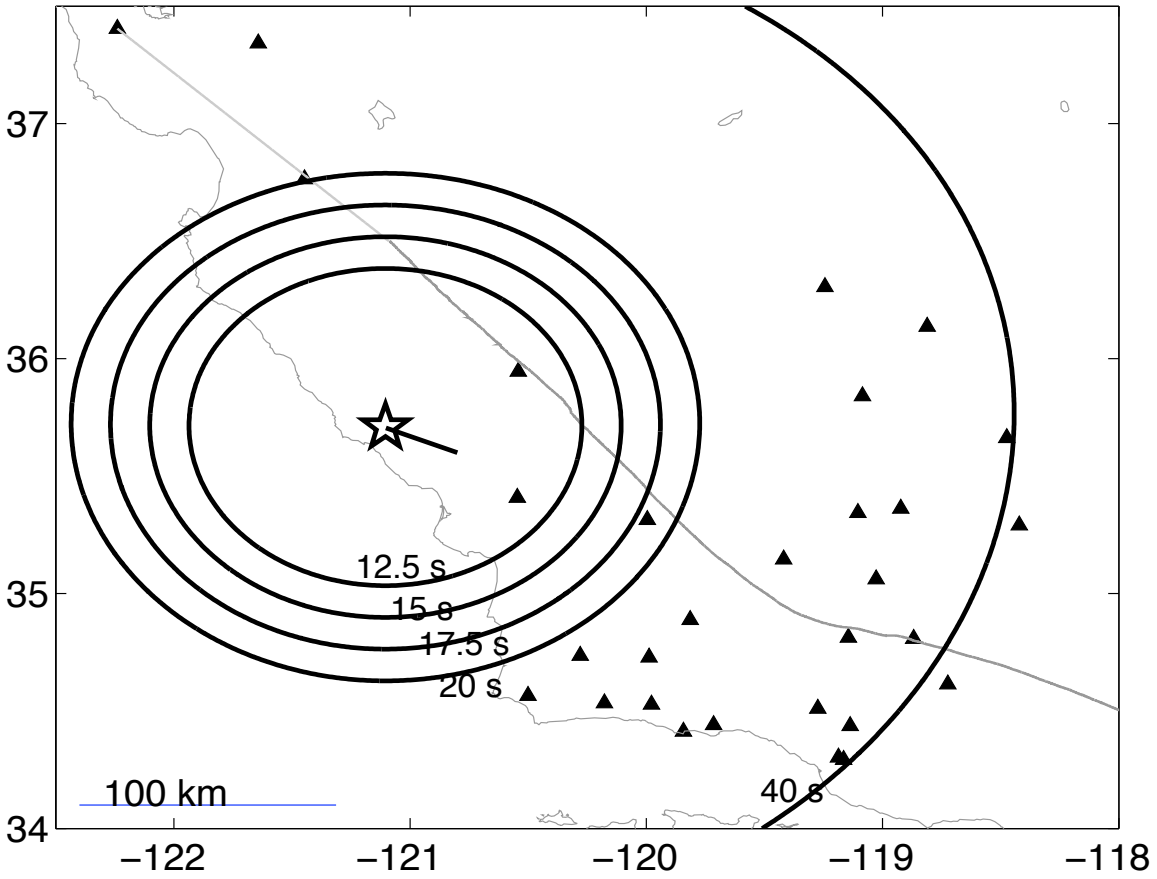

Figure 6.7: SCSN stations used to update the VS estimates for the 2003 M=6.5 San Simeon mainshock. Contours show the P-wave wavefront (for a point source at the epicenter) at the times of the VS estimates at t=3, 5.5, 8, 11, 31, 71 sec after the initial P detection; add 9.5 seconds to get VS estimate times relative to earthquake origin time, as labeled. The contour for the 71 second estimate is beyond the limits of this plot.

propagated to a third station. The initial VS estimates (t=3, 5.5, 8 sec after initial P detection at PKD or t=12.5, 15, and 17.5 seconds after origin time) will be strongly influenced by the prior information. The seismicity prior is generated by assigning locations within a 5 km radius of an earthquake in the previous 24 hours a weight of 10; all other locations have a weight of 1. The San Andreas fault prior is generated by assigning locations within 2 km of the San Andreas a weight of 10; all others have a weight of 1. The station geometry prior is generated by assigning locations within the translated edges of the first triggered station's Voronoi cell a weight of 100; all other locations have a weight of 1. These are then scaled such that they integrate to 1 over the range of possible latitude and longitudes. The location prior $prob(lat, lon)$ (Figure 6.8) is then obtained by multiplying the seismicity, San Andreas, and station geometry priors. The VS updates are calculated with and without the Gutenberg-Richter relationship. When the Gutenberg-Richter is used, the magnitude prior has the form $prob(M) = 10^{1-M}$, when it is not, the magnitude prior is $prob(M) = k$, where k is constant. Again, the magnitude prior is scaled so that it integrates to 1 over the magnitude range considered ($2 \leq M \leq 7.5$). The Bayesian prior is the product of the magnitude and location priors. That is, $prob(M, lat, lon) = prob(M) \times prob(lat, lon)$.

There were two events located by BDSN (in the Northern California catalogue) in the 24 hours prior to the San Simeon mainshock within PKD's Voronoi cell- an M=1.18 event on the San Andreas (at 2003/12/21:21:15:39.790) and an M=1.22 event within 8.5 km of the mainshock epicenter (at 2003/12/22,08:37:32.9). After the initial P detection, but before taking into account the available amplitudes, $prob(lat, lon)$ is peaked at the location of the M=1.18 event (labeled "1" in Figure 6.8) near the San Andreas and has high values at the location of the M=1.22 event (labeled "2" in Figure 6.8), as well as along the length of the San Andreas within PKD's Voronoi cell.

Given only the peak amplitudes at PKD 3 seconds after the initial P detection (no prior information, and not taking into account the P arrival or amplitudes at the second triggered station PHL), Figure 6.9 shows the locations consistent with each of 6 different magnitude ranges: $2 \leq M < 3$, $3 \leq M < 4$, $4 \leq M < 5$, $5 \leq M < 6$,

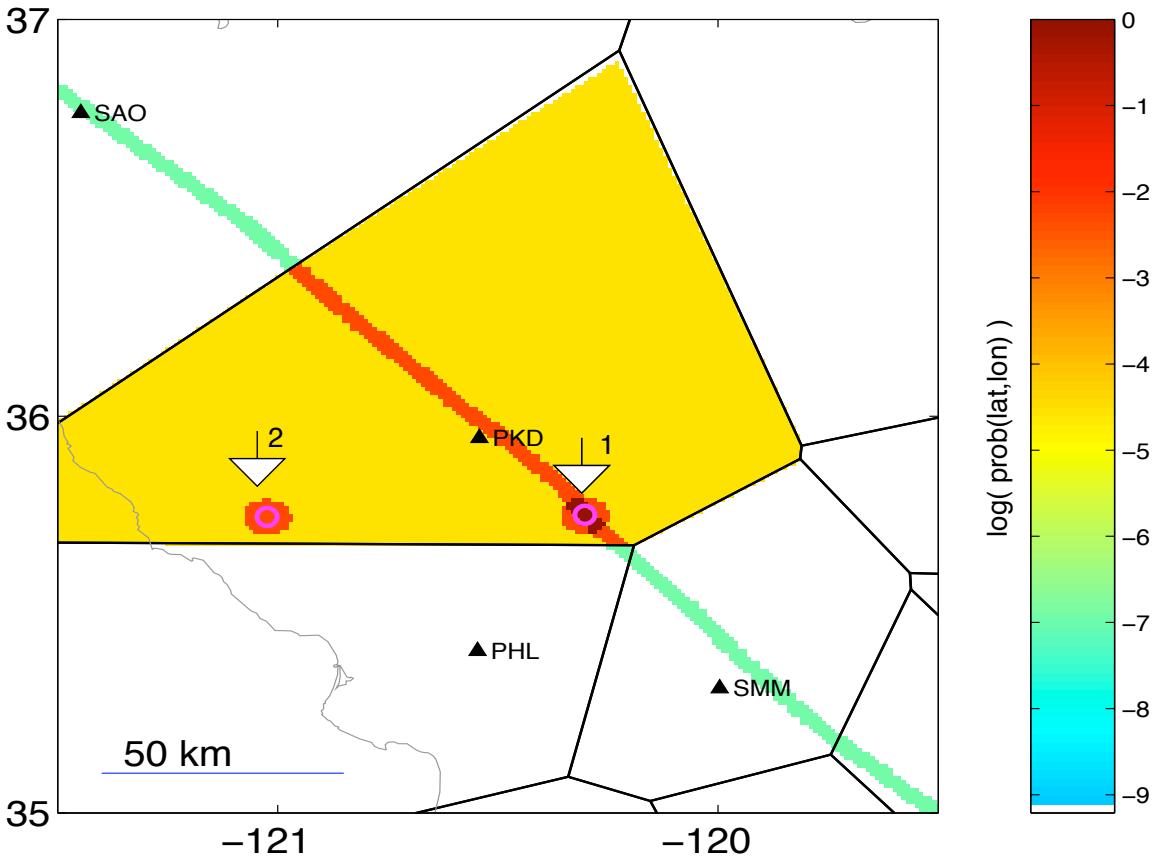

Figure 6.8: The (log of the) Bayes prior, $prob(lat, lon)$. The types of information included are: station geometry, seismicity in the preceding 24 hours, and fault location. This also takes into account that the first P arrival is detected at PKD, although this is technically an observation, and not prior information.Using the ad hoc method to account for previous seismicity and the San Andreas fault trace, $prob(lat, lon)$ is peaked at the location of the M=1.18 event on the San Andreas (1), and has high values at the location of the M=1.22 event (2), as well as along the length of the San Andreas within PKD's Voronoi cell. Using formal foreshock/aftershock statistics (Reasenberg and Jones, 1989; Gerstenberger et al., 2003), in particular, Omori's law, might mean that the location prior is peaked at (2).

$6 \leq M < 7$, and $M \geq 7$. For each magnitude range, the contours of the location marginal of the likelihood function (integrated over the given magnitude range and scaled to a maximum value of 1) are drawn at the 0.01, 0.1, and 0.6 levels. The regions where the value of the scaled location marginal is ≥ 0.6 are shaded. In general, there is much more area consistent with larger magnitudes than smaller events.

The VS estimate for magnitude and epicentral location 3 seconds after the initial P detection is a combination of the Bayes prior (Figure 6.8), the likelihood function given the available amplitudes (Figure 6.9), as well as constraints on earthquake location given the available P arrivals and non-arrivals. (The constraints from the P arrivals and non-arrivals will be discussed shortly.)

In Figures 6.10, 6.12, and 6.13, which show the VS location estimates at 3, 5.5, and 8 seconds after the initial P detection, the color scales with the probability of the event being located at that given location and the contours convey the magnitude estimates *without* the Gutenberg-Richter magnitude-frequency relationship. At 3 seconds after initial P detection at PKD, the VS estimates take into account 1) previous seismicity, 2) San Andreas fault location, 3) station geometry, 4) 1 second interval between P arrivals at PKD and PHL, 5) no P arrivals at other stations sharing Voronoi edges with PKD (SMM, SAO, RCT, and VES), and finally 6) the peak amplitudes available at PKD. Note, the amplitudes at PHL are not included in the initial estimates, since there is not yet 3 seconds worth of data at PHL. The VS estimate is an earthquake located on the San Andreas at the location of the M=1.18 that occurred within the previous 24 hours with a magnitude of $M = 5.8 \pm 0.6$ *without* G-R, and $M = 5.1 \pm 0.56$ with G-R. Both the VS current estimate and the actual location are consistent with the arrival information (P arrivals at PKD and PHL, no arrivals at SMM, SAO, RCT, and VES) and are within 5 km of an earthquake in the previous 24 hours. The 3-second VS location estimate a higher prior probability than the actual location due to its proximity to the San Andreas. In Figure 6.10, the 3-second VS location estimates are marked by a gray diamond. Both (a) and (b) show the location marginal, $prob(lat, lon|data)$, of the VS estimate; (b) is plotted on a log scale. In Figure 6.10(b), the shape of the colored region within PKD's Voronoi

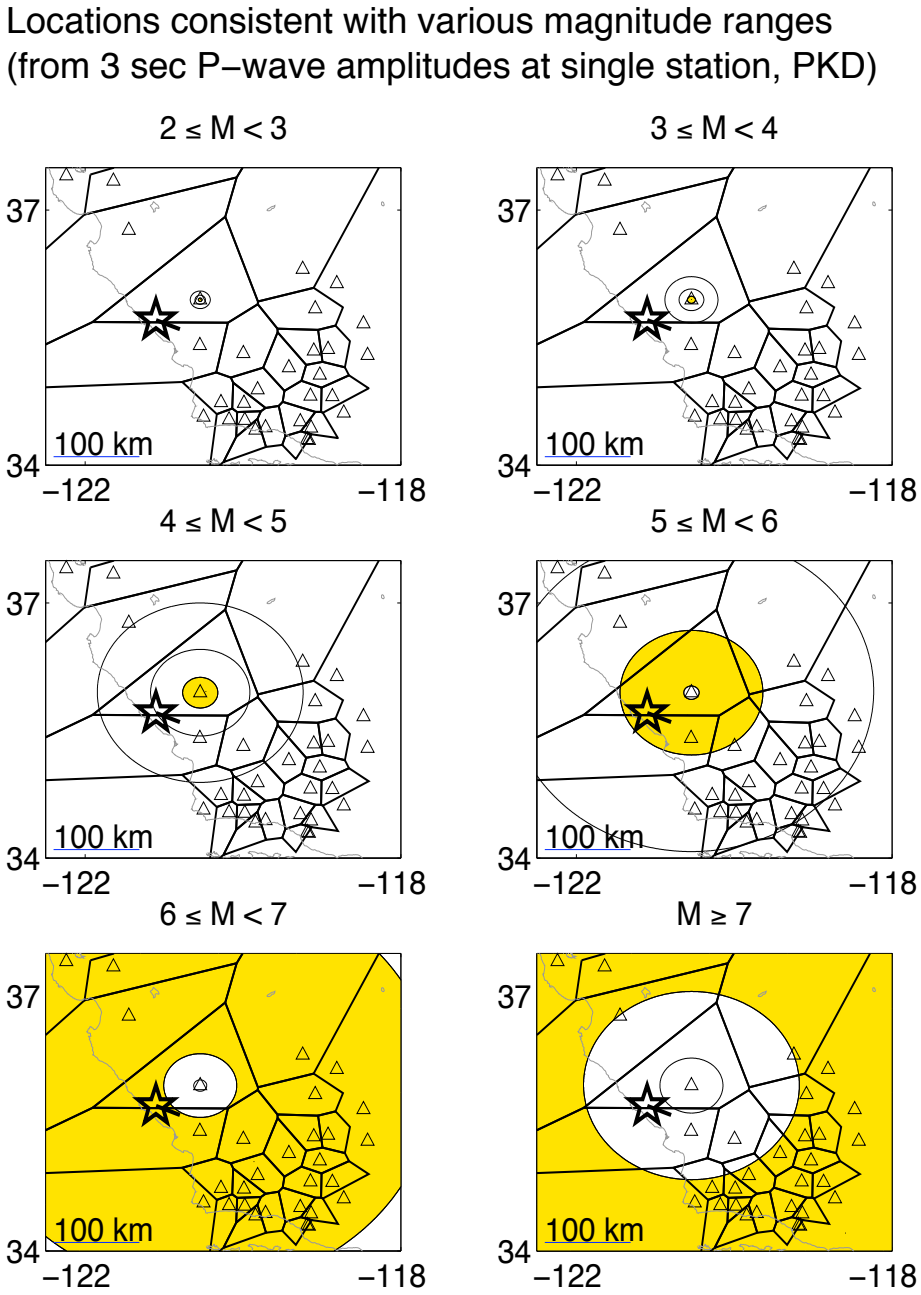

Figure 6.9: The shaded regions in each subplot are the locations consistent with the stated magnitude range given the peak P-wave amplitudes 3 seconds after the initial P detection at PKD. Note the total "high probability" shaded area consistent with $M \geq 5$ events is much larger than for $M \leq 5$ earthquakes. 3 seconds of P-wave amplitudes from the first triggered station cannot uniquely resolve the source parameters. There are trade-offs in magnitude and epicentral location, just as there were trade-offs between magnitude and epicentral distance, as shown in Figure 6.4.

cell is governed by the available P arrivals and non-arrivals. The details within this region are determined by the observed time between the arrivals at PKD and PHL, the previously observed seismicity, the San Andreas fault trace, and the 3 second amplitudes at PKD.

The VS estimate is updated 5.5 seconds after the initial P detection. At this time, there are 3 seconds worth of data at PHL, and the likelihood takes into account the amplitudes at PKD and PHL. Aside from the arrival at the second station PHL (which was accounted for in the initial estimate), there are no other arrivals at other stations. The non-arrivals are useful information. In Figure 6.11, the shaded regions are those consistent with the arrival or non-arrival information available for station PKD and each of its surrounding stations. The combination of these 6 constraints eliminate the San Andreas location as a possible location for the on-going earthquake.

At 5.5 seconds after the initial P detection, the non-arrivals (in particular, at station SMM) eliminate the location of the M=1.18 on the San Andreas as a possible location for the on-going earthquake. The VS location estimate is now at the location of the M=1.22 possible foreshock. This estimate, based on 2 P-arrivals, 4 non-arrivals, and previous seismicity, and the available amplitudes, is within 7.1 km of the epicenter reported by SCSN. The VS magnitude estimate is $M = 6.5 \pm 0.43$ without the G-R, and $M = 6.1 \pm 0.42$ with the G-R. Without the previously observed seismicity, the location estimate at this time would be the blue strip along the shared edge of PKD and PHL in Figure 6.12.

At 8 seconds after the initial P detection, a third arrival is available at SMM. The location problem is now uniquely determined. The location estimates for subsequent VS estimates do not change much; they are within 10 km of the SCSN-reported epicenter. However, the magnitude estimates for the subsequent VS estimates continue to change. At 8 seconds after the initial P detection (Figure 6.13), only the P-wave amplitudes at PKD and PHL are included; 3 seconds worth of data is not yet available at SMM. The VS magnitude estimate without the G-R is $M = 6.6 \pm 0.42$, with the G-R is $M = 6.2 \pm 0.40$.

Figure 6.14 shows the availability of observations as a function of time. For seismic

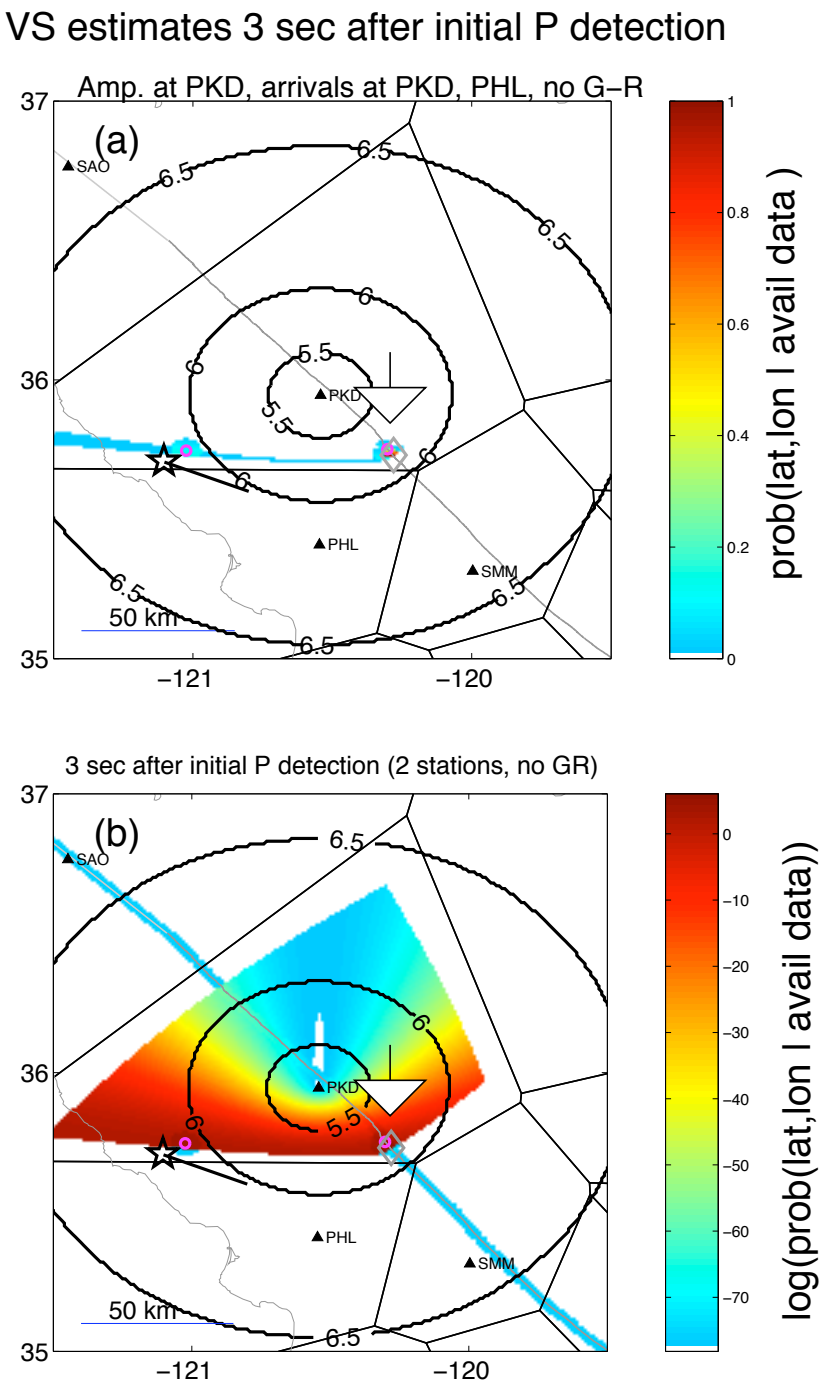

Figure 6.10: The colors correspond to the value of the location marginal of the Bayes posterior, $prob(lat, lon|data)$ (integrating out the effects of magnitude from the posterior pdf, $prob(M, lat, lon|data)$). (a) shows $prob(lat, lon|data)$, whereas (b) shows $\log prob(lat, lon|data)$. The initial VS estimate locates the on-going event at the location of the M=1.18 San Andreas event. Without the G-R, the VS magnitude estimate is $M = 5.8 \pm 0.6$, with the G-R, it is $M = 5.1 \pm 0.56$. Gray diamonds (indicated by the arrows) are the VS location estimates.

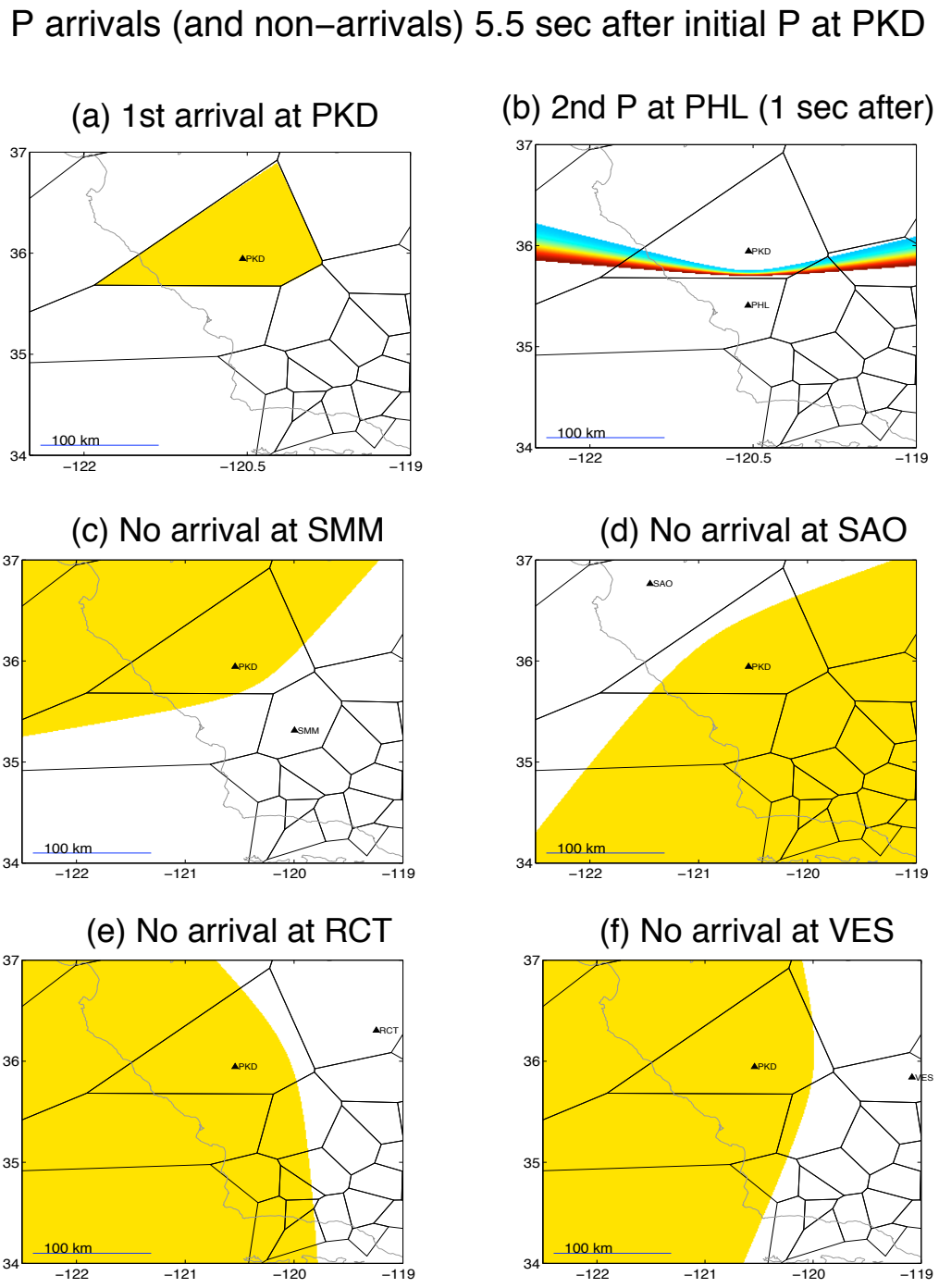

Figure 6.11: The shaded regions are those consistent with (a) the first P detection at PKD, (b) the interval of about 1 second between the arrivals at PKD and PHL, (c-f) no P arrivals at SMM, SAO, RCT, and VES, which share Voronoi edges with PKD, 5.5 seconds after the initial P arrival at PKD.

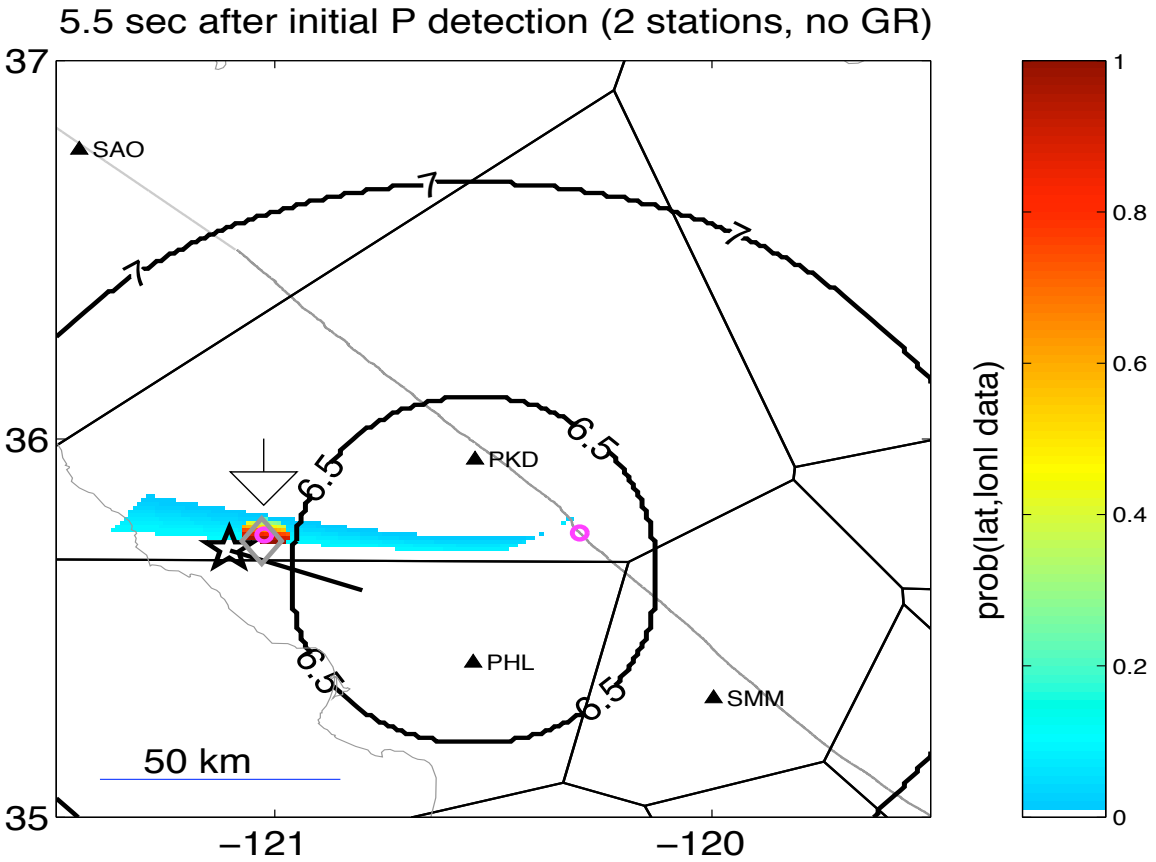

Figure 6.12: The VS estimates are updated at 5.5 seconds after the initial P detection. By this time, P arrivals and the peak amplitudes at two stations are available; the non-arrivals (in particular at SMM) eliminate the San Andreas location as a potential location. The updated VS location estimate is within 7.1 km of the actual (SCSN-reported) epicenter. The VS magnitude estimate is $M = 6.5 \pm 0.43$ without G-R, and $M = 6.1 \pm 0.42$ with the G-R.

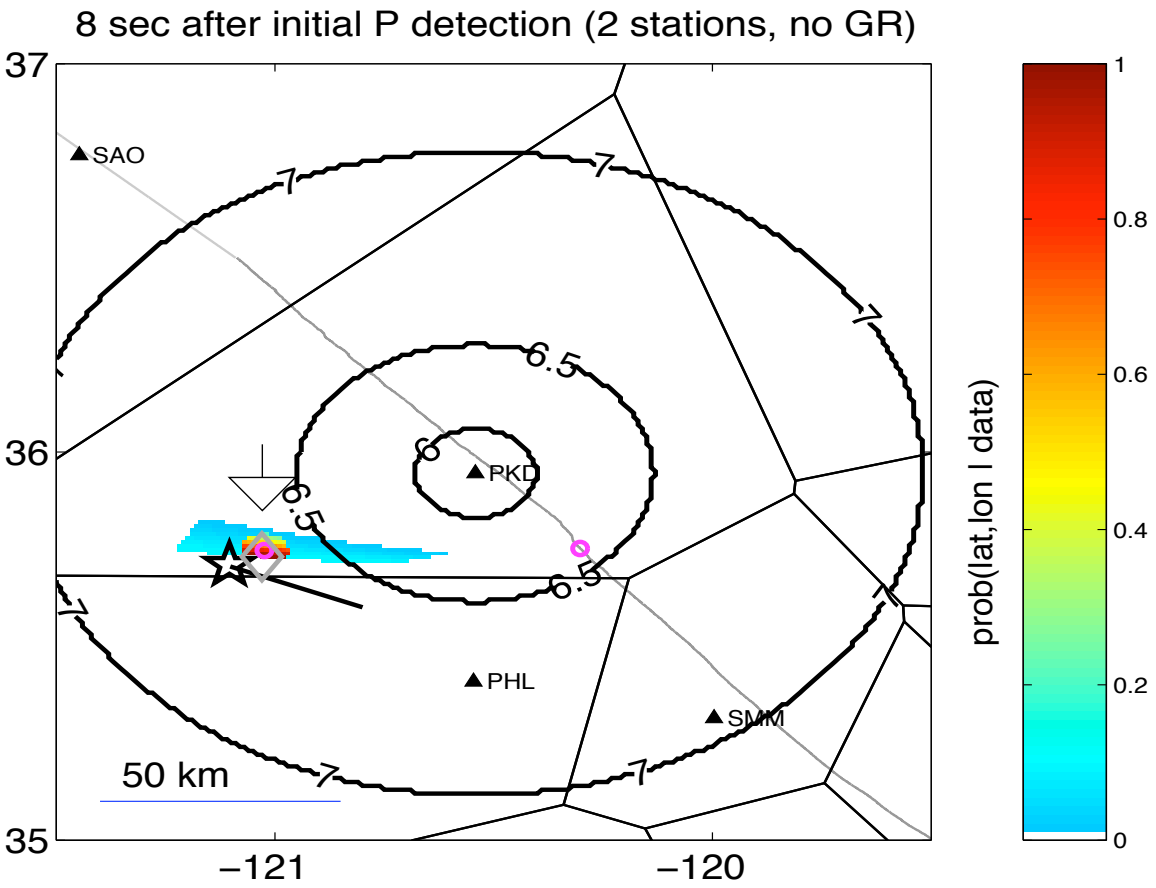

Figure 6.13: The VS estimates are updated at 8 seconds after the initial P detection. By this time, a third P arrival is available at SMM, and the location problem is uniquely determined. The VS location estimate is 7.1 km away from the SCSN-reported location. The contours shown are for the VS magnitude estimates without the Gutenberg-Richter relationship. The VS magnitude estimate without the G-R is $M = 6.6 \pm 0.42$, and with the G-R is$M = 6.2 \pm 0.42$. The observations for this estimate are P arrivals at 3 stations, non-arrivals at 3 other stations, and peak P wave amplitude information from 2 stations.

early warning, the earlier estimates are the most important. There is typically not much data in the first 10 seconds after the initial P detection. It is at this stage that the prior information is most useful. The information incorporated into the Bayes prior includes 1) station geometry, 2) previously observed seismicity, and 3) the San Andreas fault trace. The uncertainty in the VS estimates decreases as $\frac{1}{\sqrt{N}}$ (since observations are assumed independent), where N is the number of stations contributing data. Figure 6.15 shows the magnitude estimates as a function of time. The uncertainties are initially large, and decrease like $\frac{1}{\sqrt{N}}$. The VS estimates including the Gutenberg-Richter relationship in the Bayes prior is slower to approach the SCSN-reported magnitude than the other estimates. Figure 6.16 shows the evolution of the VS location estimates as a function of time. The VS location estimate is within 10 km of the SCSN-reported location at 5.5 seconds after the initial P detection. This estimate is based on 2 P arrivals at PKD and PHL, non-arrivals at stations SMM, SAO, RCT, and VES, as well as the constraints of previously observed seismicity. As shown in Figure 6.12, without the previous seismicity, the location estimate at 5.5 seconds would be a strip of about 100 km between PKD and PHL.

The VS estimates at 80 seconds after the origin time are not useful for seismic early warning, since the large ground motions have by now propagated to the areas that would have had strong shaking (see Figure 6.7). However, the VS estimates (using a uniform prior) at large t after the origin time provide amplitude-based location estimates. Figures 6.17 and 6.18 compare the arrival- and amplitude-based location estimates at 31 and 71 seconds seconds after the initial P detection (or 40 and 80 seconds after the origin time). The arrival-based estimates are obtained by minimizing the difference between the predicted and observed P wave arrival times. In Figure 6.17 and 6.18, the arrival-based estimates are based on 31 observed P arrivals. The difference in these two Figures is the amount of data included in the amplitude-based estimates. In Figure 6.17, the amplitude-based locations are based on the distribution of 31 P-wave amplitudes and 5 S-wave amplitudes. There is agreement between the arrival- and (predominantly P-wave) amplitude-based estimates. In Figure 6.18, the amplitude-based locations are based on the distribution of 31 P-wave amplitudes and

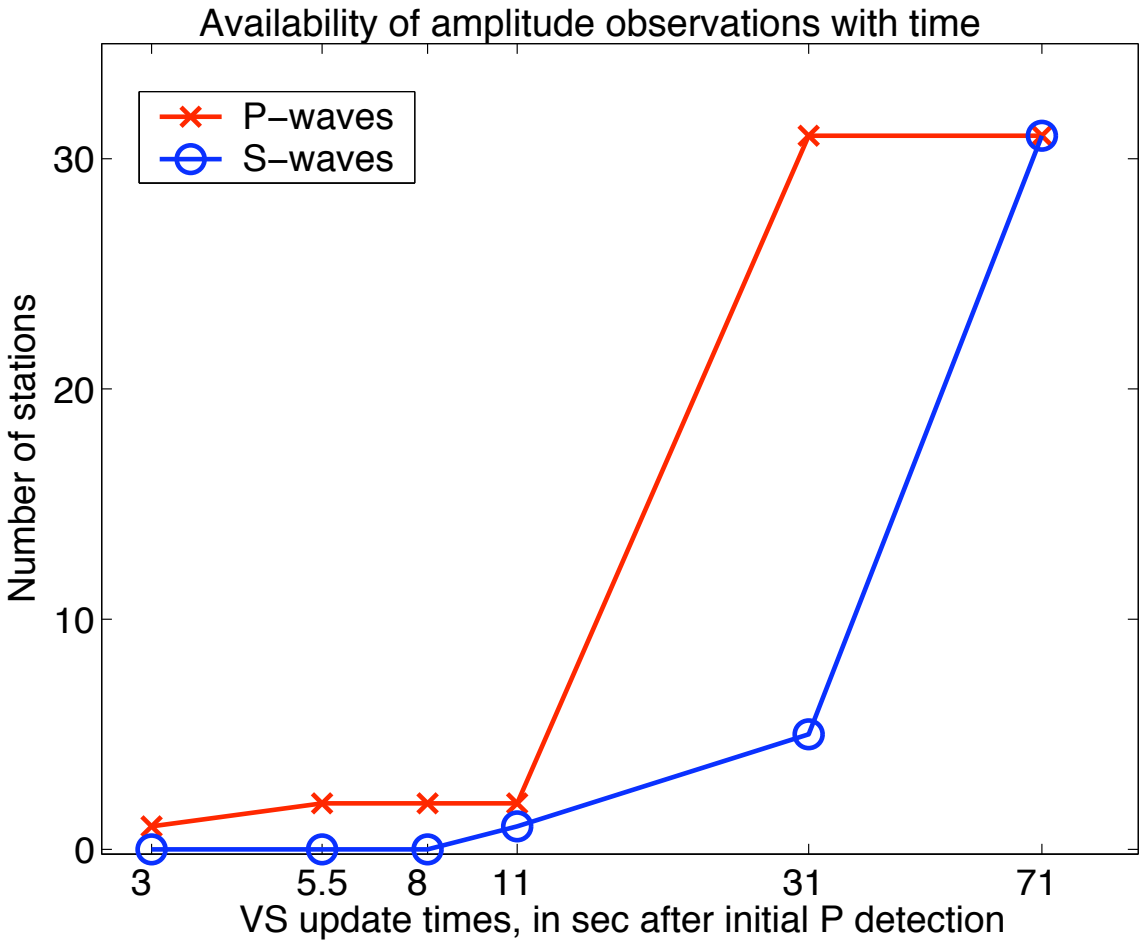

Figure 6.14: The number of stations contributing P and S wave amplitudes to the VS estimates as a function of time. When the set of available observations is sparse (the first 4 VS estimates), the prior information is relatively influential. The prior information included in this analysis are: station geometry, previously observed seismicity, the San Andreas fault trace, and the Gutenberg-Richter magnitude-frequency relationship.

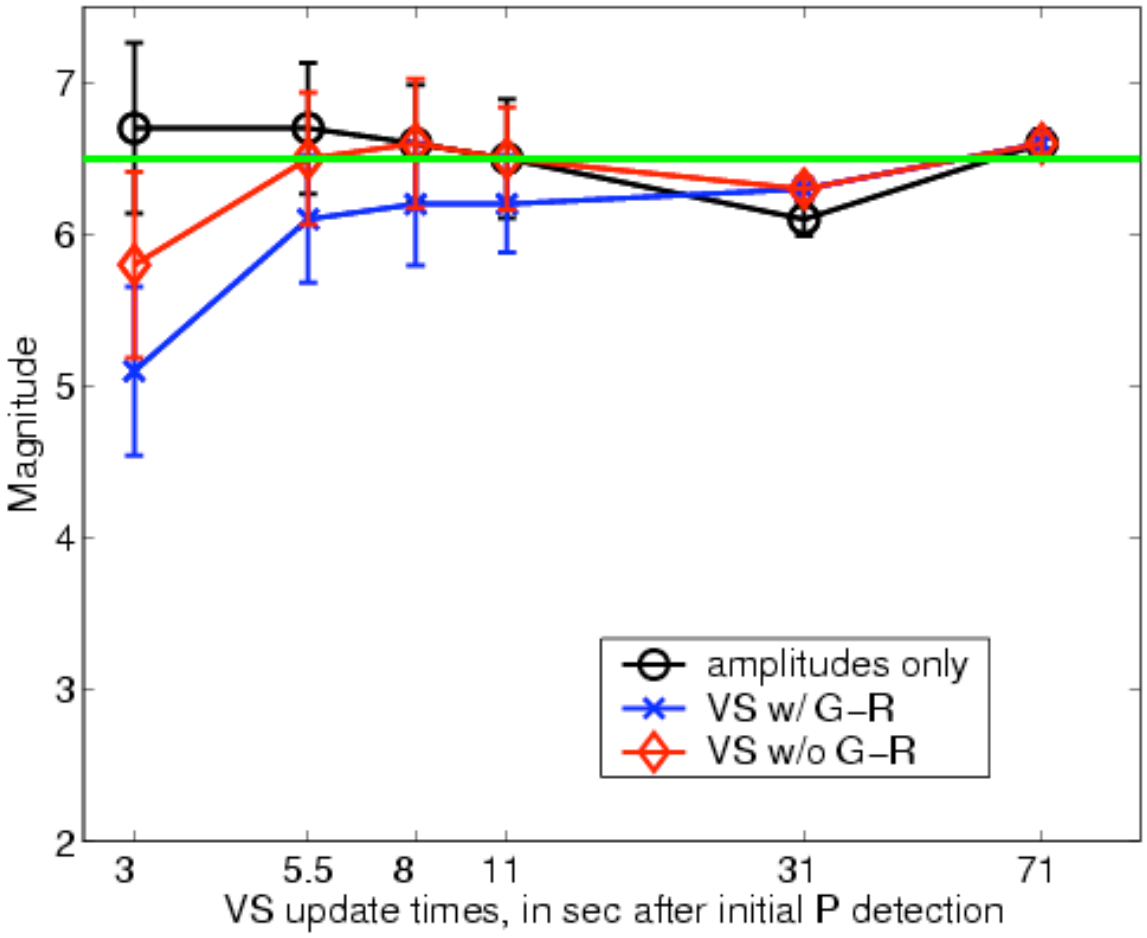

Figure 6.15: The evolution of various magnitude estimates as a function of time. The estimates labeled "amplitude only" correspond to not using any prior information. The VS magnitude estimates with and without the Gutenberg-Richter relationship in the Bayes prior are shown. The horizontal line denotes the SCSN-reported magnitude of M=6.5. The VS estimates without the G-R approach the SCSN-reported magnitude faster than those with the G-R in the Bayes prior.

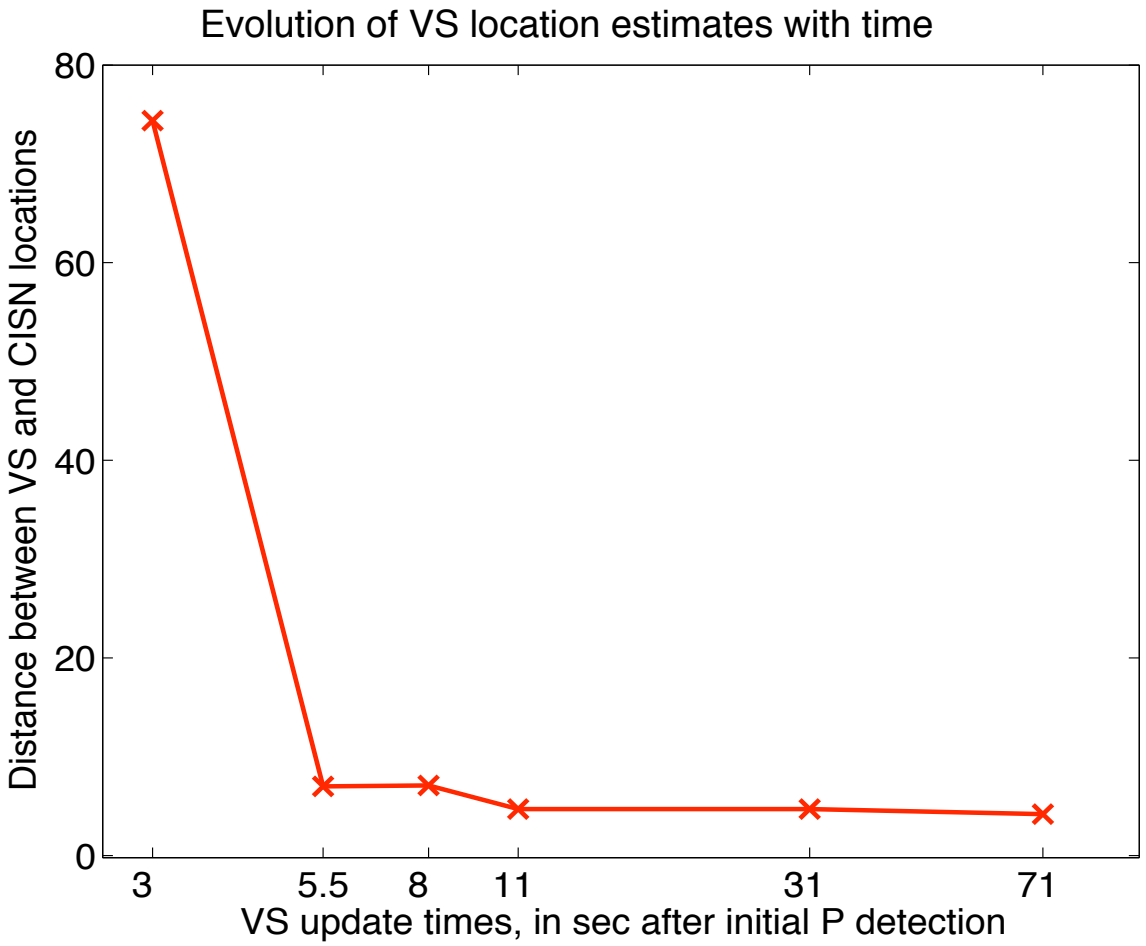

Figure 6.16: The evolution of VS location estimates as a function of time. Plotted are the distance between the VS location estimate and the SCSN-reported location. Note that the SCSN location is typically based on numerous arrivals and waveforms; these are available about 30 seconds after the initial P detection. The VS estimates are based on the available data as shown in Figure 6.14. The VS location estimate is within 10 km of the SCSN location with at 5.5 seconds after the initial P detection (with only 2 P arrivals). At 80 seconds after the origin time (71 seconds after the initial P detection), the VS location estimates are within 5 km of the SCSN location.

31 S-wave amplitudes. The contours of the arrival- and amplitude-based estimates do not overlap. A possible explanation is that the relatively high density of stations to the southeast coincide with a maximum of the S-wave radiation pattern. This combination introduces strong positive correlations in the observed S-wave amplitudes to the southeast. The VS method, which uses a point-source model and does not account for radiation pattern, directivity, or finite faults. It compensates for such factors by moving the location closer to the stations which experience these effects.

Figures 6.19 and 6.20 show how the envelope attenuation relationships derived in Chapters 2 and 3 compare with the peak horizontal S-wave amplitudes and the peak vertical P wave amplitudes. In general, the envelope attenuation relationships adequately describe the observed amplitudes. Note that the San Simeon records were not included in the dataset from which these envelope attenuation relationships were derived. Figure 6.21 shows the magnitude estimates based on P- and S-wave vertical ground motion ratios as a function of distance. There is no apparent distance-dependence in the ratio-based magnitude estiamtes.

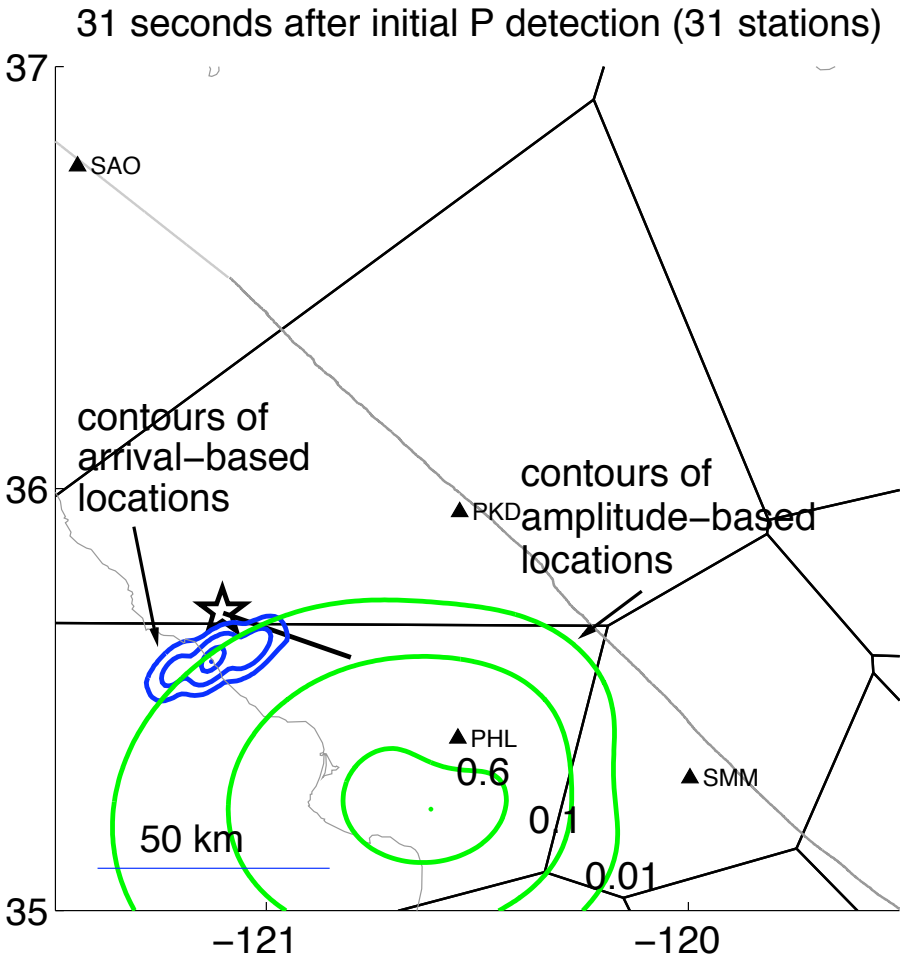

Figure 6.17: Comparison of amplitude- and timing-based location estimates 40 seconds after the initial P detection. The amplitude-based location is based on the distribution of 31 P-wave amplitudes and 5 S-wave amplitudes. The timing-based location is obtained by minimizing the residual between the predicted and observed arrival times give 31 P-wave arrivals. There is a general agreement between these two solutions, which are relatively independent of each other since they are based on different observations.

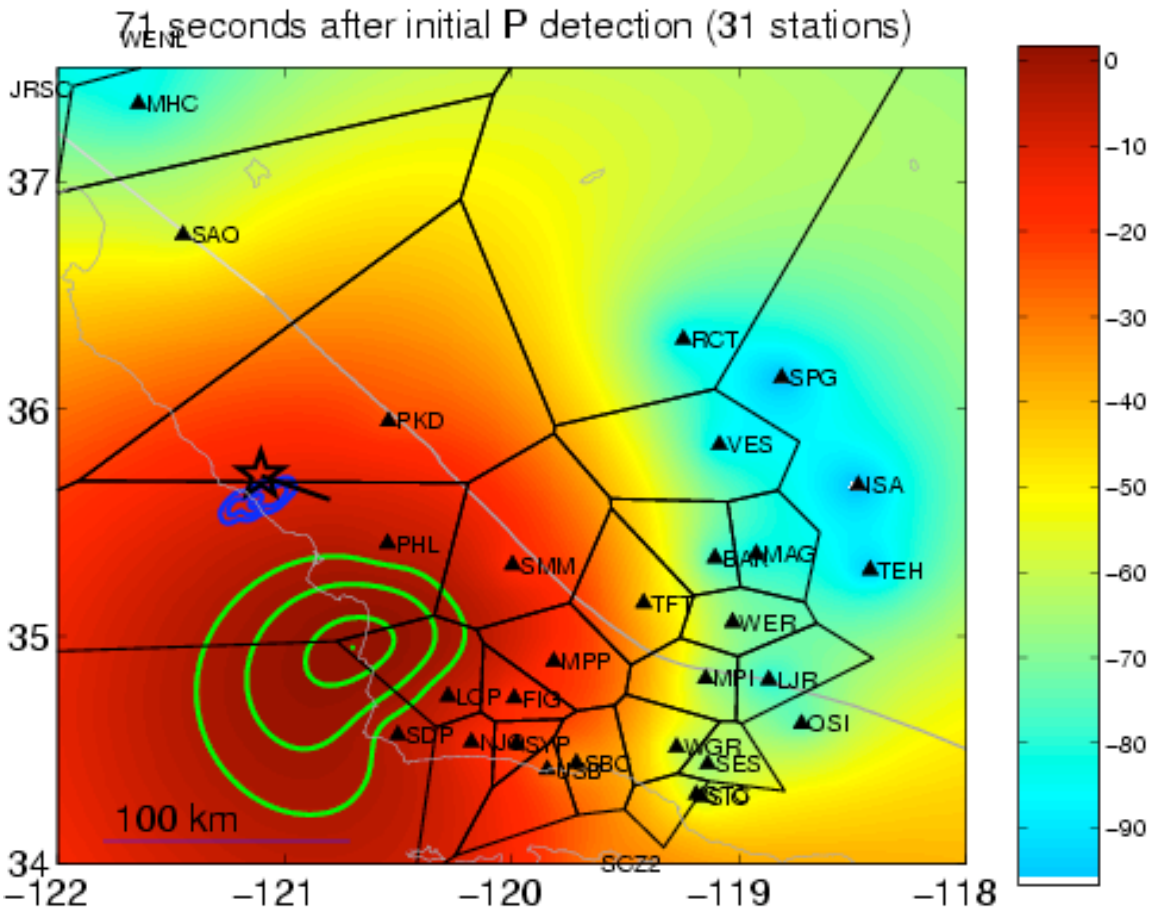

Figure 6.18: Comparison of amplitude- and timing-based location estimates 80 seconds after the initial P detection. The amplitude-based locations are derived from the distribution of 31 P-wave amplitudes and 31 S-wave amplitudes. The timing-based location is based on 31 P-wave arrivals and is the same timing-based solution shown in Figure 6.17. The amplitude- and timing-based locations no longer agree. A possible explanation is that the cluster of stations to the southeast coincide with a maximum of the S-wave radiation pattern, a combination which would result in strong positive correlations in the observed S-wave amplitudes in the southeast direction. Effects such as directivity, radiation pattern, and finite faults, are not accounted for by the VS method, which is a point-source characterization.

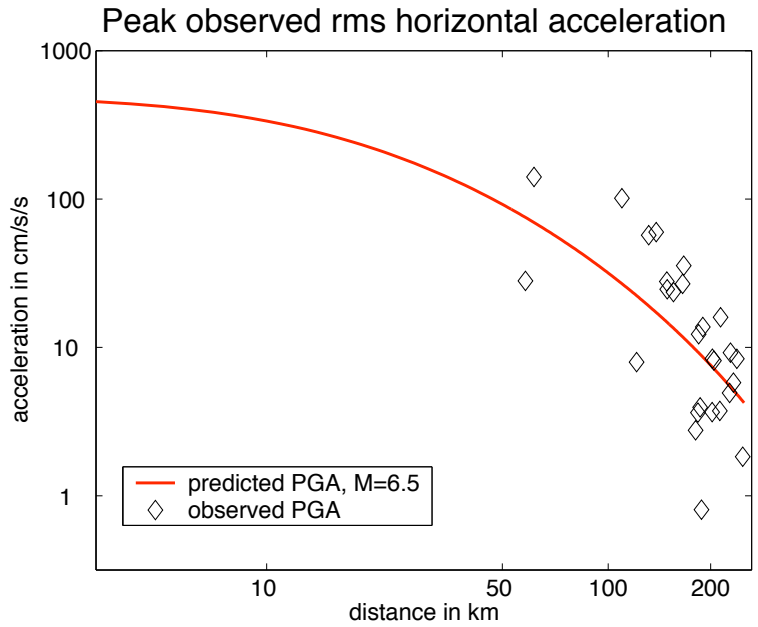

(a)

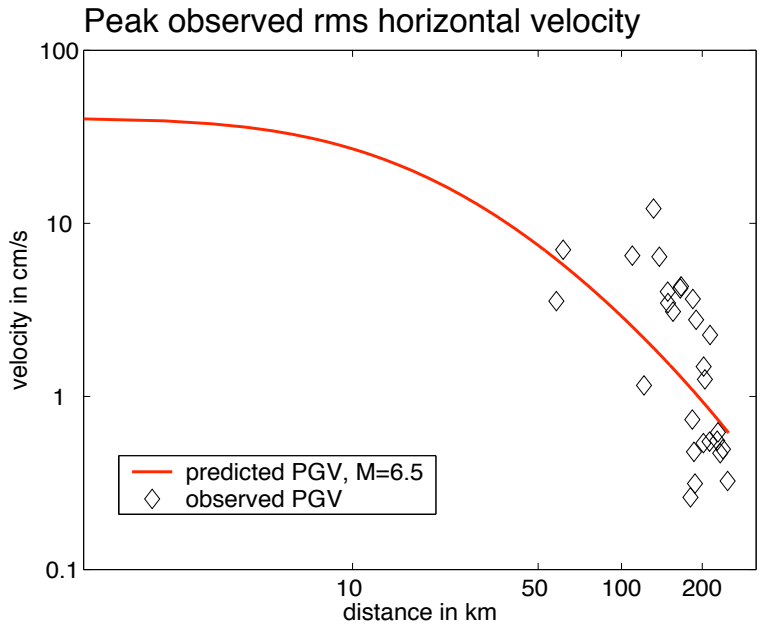

(b)

Figure 6.19: The predicted ground motion levels as a function of distance given by the envelope attenuation relationships developed in Chapter 2 for an M=6.5 earthquake and the observed root mean square of the peak horizontal S-wave ground motion (a) acceleration and (b) velocity amplitudes.

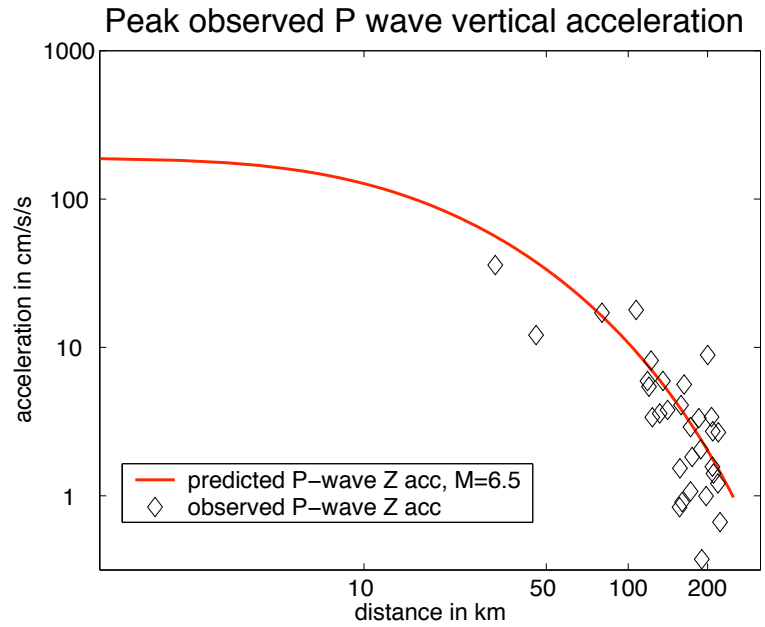

(a)

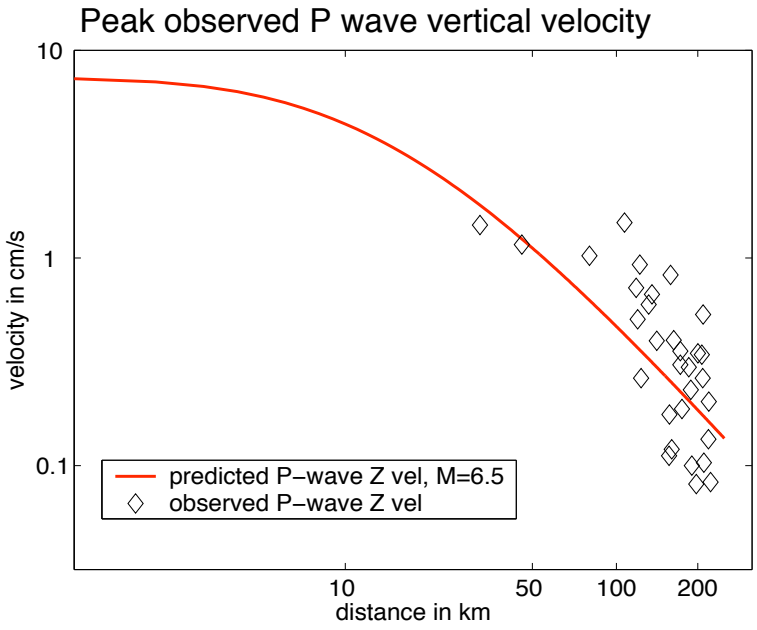

(b)

Figure 6.20: The predicted vertical P-wave amplitudes as a function of distance given by the envelope attenuation relationships developed in Chapter 2 for an M=6.5 event and the observed peak vertical P-wave amplitudes for ground motion (a) acceleration and (b) velocity.

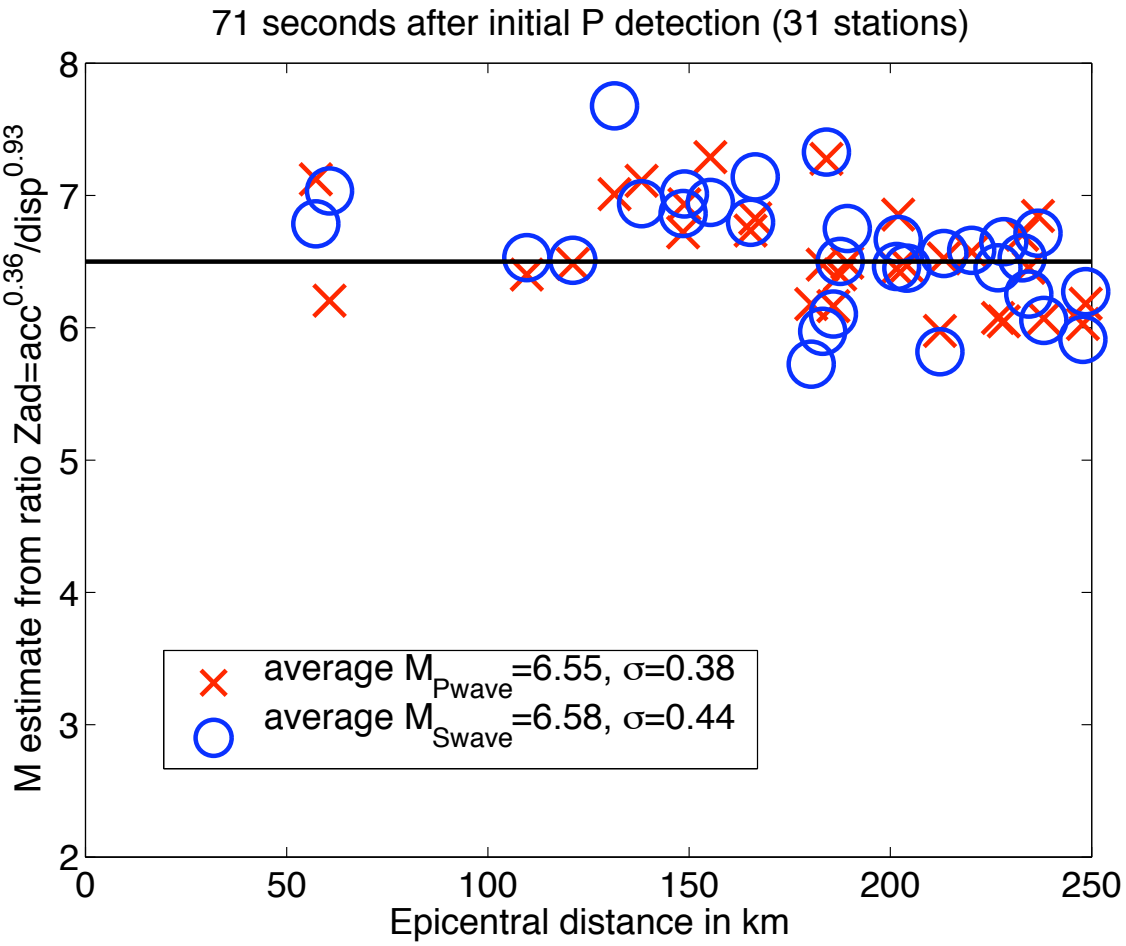

Figure 6.21: Magnitude estimates based on the vertical ground motion ratio, $Zad = acc^{0.36}/disp^{0.93}$, for P- and S-waves as a function of distance. The horizontal line is the SCSN-reported magnitude of M=6.5. If there is a distance-dependence in the ratio-based magnitude estimates, it is very slight. The average S-wave estimate is slightly larger than the average P-wave estimate; in the other events examined, the S-wave magnitude estimates are usually lower than those from the P-wave. This may be due to directivity effects.